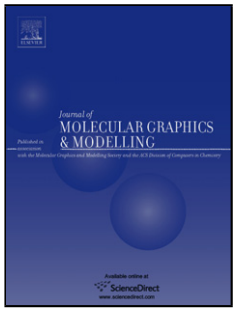

Title: π-stacking effects on the hydrogen bonding capacity of methyl 2-naphthoate

Author: Farideh Badichi Akher Ali Ebrahimi

PII: S1093-3263(15)30019-X
DOI: http://dx.doi.org/doi:10.1016/j.jmgm.2015.06.013
Reference: JMG 6568

To appear in: *Journal of Molecular Graphics and Modelling*

Received date: 16-1-2015
Revised date: 22-6-2015
Accepted date: 24-6-2015

Please cite this article as: Farideh Badichi Akher, Ali Ebrahimi, *rmpi*-stacking effects on the hydrogen bonding capacity of methyl 2-naphthoate, Journal of Molecular Graphics and Modelling http://dx.doi.org/10.1016/j.jmgm.2015.06.013

π-stacking effects on the hydrogen bonding capacity of methyl 2-naphthoate

Farideh Badichi Akher, Ali Ebrahimi *

Department of Chemistry, Computational Quantum Chemistry Laboratory, University of Sistan and Baluchestan, P.O. Box 98135-674, Zahedan, Iran

ebrahimi@hamoon.usb.ac.ir (A. Ebrahimi)

*Corresponding author E-mail: ebrahimi@hamoon.usb.ac.ir (A. Ebrahimi)
Fax: +98-541-2446565

Graphical abstract

fx1

Highlights

- Interplay between π-stacking and hydrogen bond interactions in the fused two-ring system (methyl 2-naphthoate) have been evaluated by computational quantum chemistry methods.
- All substituents enhance the stacking interactions relative to the unsubstituted case, where enhancement is higher for electron-withdrawing substituents.
- The hydrogen bonding ability of lone pairs of O* atom of stacked MNP decreases in the presence of strong electron-withdrawing substituents (NO_2, NO and CN).
- Two correlation equations were found for prediction of the ΔE values of the binary stacked Ph-X||MNP complexes, one based on the combination of the σ_{meta}, σ_{para}, and MR values and another based on the topological properties of electron charge density.
- The H-bonding ability can be related to the sum of local minima of ESPs calculated between rings in the binary stacked Ph-X||MNP complexes.

Abstract

π-stacking effects of fused two-ring system of methyl 2-naphthoate (MNP) with benzene derivatives on the -CO group, as a hydrogen bond acceptor, has been investigated by the quantum mechanical calculations at the M06-2X/6-311++G(d,p) level of theory. All substituents enhance the stacking interactions relative to the unsubstituted case, where enhancement is higher for

electron-withdrawing substituents (EWSs). The hydrogen bonding ability of lone pairs of O* atom of stacked MNP decreases in the presence of strong electron-withdrawing substituents (NO_2, NO and CN). The hydrogen bond ability of -CO group of MNP is related to the sum of local minima of electrostatic potentials (∑ESPs) observed between stacked rings. The charge transfer (CT) is lower in the presence of EWSs. The study also shows that the interaction energies (ΔE) are linearly dependent on the combination of the sum of electron densities calculated at the bond critical points (BCPs) between the rings ($\sum\rho_{BCP}$) and the sum of electron charge densities calculated at the ring critical points ($\sum\rho_{RCP}$). There are good relationships between the Hammett constant σ_{meta} and the global minimum of electrostatic potential around the O* atom (V_{min}), the sum of local minima of the electrostatic potentials obtained between stacked rings, and the results of natural population analysis (NPA). An excellent correlation was found between the ΔE values and a combination of the electrostatic (σ_{meta}), resonance/induction (σ_{para}) and dispersion/polarizibility (molar refractivity, MR) substituent constant terms.

Keywords: π-stacking, hydrogen bonding, electrostatic potential, AIM analysis, NPA analysis

Introduction

Noncovalent interactions, such as hydrogen bonding, π-stacking, etc. play an increasingly important role in supramolecular chemistry, base-to-base stacking in DNA/RNA, drug-receptor interactions, drug design, and biological structures [1-6]. π-π stacking is frequently accompanied by the hydrogen bonding in biomolecules, so, studying the effect of π-stacking on the hydrogen bonding capacity can give valuable insights on drugs and biomolecules. Several theoretical studies

have previously been performed on the effect of π-stacking on the hydrogen bonding capacity [7-9].

Mignon and coworkers [7] investigated the influence of stacking on the hydrogen bonding of an aromatic nitrogen base (pyridine). They found that the hydrogen bonding capacity of the N atom of pyridine is directly related to the electrostatic interaction between the rings. On the other hand, the basicity of pyridine increases with increasing the electron-donating (ED) character. Mignon and coworkers [8] also studied the influence of stacking of substituted benzenes upon the hydrogen bonding ability of stacked pyrimidine and imidazole in three cases including T-shaped, parallel-displaced and parallel-sandwich cases. Once again, it was confirmed that the electrostatic interaction between the rings has a direct relationship with the hydrogen bonding ability of the heterocycles, and dispersion forces play an important role in the stabilization of the complexes. In the parallel stacking arrangement, all substituents increased the hydrogen bonding capacity of both pyrimidine and imidazole relative to the unsubstituted case (X = H), where the effect was higher with EWSs. Also, the hydrogen bonding capacity of the pyrimidine base was estimated higher than imidazole in the parallel stacked arrangement. Moreover, the effect of the stacked substituted benzenes on the hydrogen bonding ability of the stacked cytosine has been investigated in the offset parallel conformation [9]. The results showed that the hydrogen bonding ability of cytosine increased with increasing CT from the benzene to the stacked cytosine. On the other hand, a linear correlation has been observed between the hydrogen bonding ability of stacked cytosine and the electrostatic repulsion between the rings.

Two fused six membered rings is an important unit of drugs that can bind to the active site of a target via different interactions, including π-stacking and hydrogen bonding of -CO group as a hydrogen bond acceptor. Naphthoate derivatives, which include two fused six membered rings,

are widely employed as drugs in medicine and as ligand in coordination chemistry [10-12]. Thus, interplay between π-stacking and hydrogen bond interactions in the above mentioned system can be very important in drug design efforts. In the present work, the influence of the π-stacking interaction of substituted benzenes (Ph-X, where X is NO_2, NO, COOH, SH, CN, Cl, NH_2, OH and OCH_3) with fused six membered system of methyl 2-naphthoate (MNP) on the hydrogen bond ability of -CO group of MNP have been investigated at the M06-2X/6-311++G(d,p) level of theory. The minimum on the surface of electrostatic potential of the binary stacked Ph-X||MNP complexes (BSCs) (|| donates π-stacking interaction) was used to study the interplay between these two interactions. In order to clearly investigate the hydrogen bond ability of the carbonyl group of MNP, the hydrogen bonding interaction at the carbonyl group was examined using the HF molecule in MNP and BSCs. Then the binary hydrogen bonded MNP···HF complex (BHC) was compared with the ternary stacked hydrogen bonded Ph-X||MNP···HF complexes (TSHCs). Herein, correlation of the interaction energies with the Hammett constants σ, the electrostatic potential (ESP) calculated around the O* atom of MNP, and results of the natural population analysis (NPA) and the atoms in molecules (AIM) analysis have also been investigated. The results that is obtained using BSCs simple model can be helpful in the novel drug design.

Computational details

Geometries of monomers were optimized using the hybrid meta exchange-correlation functional M06-2X [13] method in conjunction with the 6-311++G(d,p) basis set by the Gaussian09 program package [14]. Instead of full optimization of BSCs, the potential energy surface scans were performed using the single point calculations at the M06-2X/6-311++G(d,p) level of theory to ensure that the interaction between two units is through π-stacking. Thus, only isolated molecular

species were verified to be minima from frequency analysis. The initial structures of BSCs were generated by aligning the center of ring of Ph-X (X = NO_2, NO, COOH, SH, CN, Cl, NH_2, OH and OCH_3) and the center of ring II of MNP (see scheme 1). To determine the largest interaction energy, six parameters were considered: D1 for vertical separation, α for rotation angle, and D2 to D5 for horizontal displacements. First, the preferred D1 was determined by 0.1 Å increments then it was held fixed for the remaining calculations, where the ring of Ph-X was rotated in 30° (6 steps of size 5°) for α increments in left- and right-handed sense around the axis that passes through the centers of rings. Using the optimal D1 and α values obtained for each complex, the optimal values of D2, D3, D4 and D5 were obtained upon the shift of Ph-X across the face of MNP in 0.1 Å increment. The most stable BSCs were found by comparison of the ΔE values in the optimal D2, D3, D4 and D5. All above mentioned steps have been carried out for each BSC variables.

On the other hand, to investigate the π-stacking effects on the hydrogen bonding capacity of MNP, the H-bond interaction at the carbonyl group was examined using the HF molecule. There are two orientations A and B for interaction of the HF molecule via hydrogen bonding to MNP (see scheme 1). To ensure that the interaction between the BSC and HF is mainly via the O*···H H-bond, the orientation B was selected for the O*···H interaction, where the minimum was also confirmed by frequency calculations after optimization at the M06-2X/6-311++G(d,p) level of theory.

The orientation of two rings in structure of each BSC were kept fixed and TSHCs were optimized at the above mentioned level.

The previous studies have indicated that the M06-2X functional provides a satisfactory description of noncovalent interactions in comparison with other density functionals [15]. The basis set superposition error (BSSE) was accounted through the counterpoise method [16] to correct the interaction energies of the complexes. Topological properties of the electron charge density were

calculated by the AIM method using the AIM2000 program package [17] at the M06-2X/6-311++G(d,p) level of theory. To evaluate the dipole moment of C=O* bond in MNP, the donor-acceptor interaction energy (E^2) of the lpO* → σ*HF interaction and the atomic charges in the complexes, the NPA [18] has also been performed at the M06-2X/6-311++G(d,p) level of theory by the NBO3.1 [19] program. Moreover, the local minima of the electrostatic potentials between rings and global minimum of electrostatic potential (electrostatic potential around the O* atom of the stacked MNP), as a measure of its hydrogen bonding capacity were calculated by Multiwfn 3.2 package [20].

Results and discussion

Stacking interactions between Ph-X and MNP were calculated as a function of six variables (D1, α, D2, D3, D4 and D5). After changing D1 and α, the most stable geometries of BSCs were obtained from comparison of the energy values at the optimal values of D2, D3, D4 and D5 variables. The most stable complexes correspond to the optimal D5. The graphs of the various scans are available in supplementary material. In order to investigate the interplay of π-stacking and hydrogen bond interactions, the effect of a series of substituents installed on the benzene molecule were considered on the basis of different indexes. The interaction energies (ΔE) calculated at the M06-2X/6-311++g(d,p) level of theory and corrected for BSSE, are reported in Table 1. As can be seen, the ΔE values decrease by 1.20-1.97 and 2.21-2.89 kcal mol^{-1} with BSSE correction for BSCs and TSHCs, respectively. The order of binding energies is H < OCH_3 < OH < NH_2 < Cl < SH < CN < COOH < NO < NO_2. The highest and lowest interaction energies correspond to the Ph-NO_2||MNP and Ph-H||MNP complexes, respectively. All substituents regardless of their EW or ED character enhance the magnitudes of the stacking interactions relative

to the unsubstituted case (X = H) and increasing is higher for EWSs. Such a result is contrary to the Hunter-Sanders model [21]. On the basis of that model, ED substituents (EDSs) enhance the negative charge of the π-electron clouds and thus lead to increase the repulsion (less favorable electrostatic interactions). Recently, the high-level theoretical results are at odds with Hunter-Sanders model, so the electrostatic interactions alone are not sufficient to predict the trend of the π-stacking interaction energies [22].

Relationship between the ΔE values and the Hammett constant σ_{meta}, which can describe the electrostatic effects, was investigated in BSCs. A linear correlation was not observed for ΔE–σ_{meta} pair, because both ED and EW substituents increase the stability of the complexes. Recently, Lewis and coworkers [23] studied the face-to-face interactions in X–benzene‖benzene where X–benzene was either a mono- or multisubstituted one. The results showed that there is no correlation between the ΔE and $\sum\sigma_{meta}$ values, while a reasonably good correlation was found between the ΔE and $\sum|\sigma_{meta}|$ values. They believed that the $|\sigma_{meta}|$ values contain information about the electrostatic and dispersion/polarizability of substituents and can predict the binding energies. Herein, a good linear correlation was also observed between the π-stacking interaction energies and $|\sigma_{meta}|$ (R = 0.93, with the exception of CN). With respect to suggestion of Lewis and his coworker, the correlation between the ΔE values and a combination of electrostatic substituent constant σ_{meta} and also the dispersion/polarizibility substituent constant MR was investigated in the present work. But, no suitable relationship was observed between the π-stacking interaction energies of BSCs and mentioned constants. So, other parameter may affect the stability of BSCs in addition to σ_{meta} and MR. An excellent correlation was observed between the ΔE values and a combination of the σ_{meta}, σ_{para}, and MR values on the basis of the following equation

$$\Delta E = 3.20(\sigma_{meta})^2 + 0.978(\sigma_{para})^2 - 9.3\times10^{-3}\,(MR)^2 - 1.22(\sigma_{meta} \times \sigma_{para} \times MR) - 6.23 \qquad (1)$$

The σ_{meta}, σ_{para}, and MR values were obtained from a standard reference [24]. The equation 1 can be used to predict the π-stacking interaction energies (ΔE_{pred}) of BSCs. The plot of ΔE_{pred} versus the calculated ΔE shows a reasonably good correlation (see Fig. 1, R = 0.97).

On the other hand, to investigate the π-stacking effects on the hydrogen bonding capacity of MNP, the ΔE values of the O*···H interaction in BHCs and TSHCs have been calculated at the M06-2X/6-311++g(d,p) level of theory. The trend in the interaction energies of TSHCs is H < OH < OCH_3 < Cl < NH_2 < CN < SH < COOH < NO < NO_2. As can be seen, the highest and lowest interaction energies correspond to the Ph-NO_2||MNP and Ph-H||MNP complexes, respectively. Both the EW and ED substituents increase the magnitudes of the interactions energies relative to the unsubstituted case (X = H) and increasing is higher for EWSs. The relationship between the ΔE values of the O*···H interaction in TSHCs and σ_{meta} (and $|\sigma_{meta}|$) was also investigated, but no correlation was observed between them. Similar to equation reported for BSCs, a three variable equation with a combination of the σ_{meta}, σ_{para}, and MR values was found for estimation of the ΔE values of the O*···H interaction in TSHCs with an excellent correlation (see Fig. 1, R = 0.96).

$$\Delta E = 3.28(\sigma_{meta})^2 + 0.45(\sigma_{para})^2 - 0.01(MR)^2 - (\sigma_{meta} \times \sigma_{para} \times MR) - 15.34 \quad (2)$$

The $R_{O^{*}\cdots H}$ geometry parameter can be used to determine the strength of hydrogen bonding in TSHCs. According to Table 1, it is obviously found that the $R_{O^{*}\cdots H}$ increases in the presence of EWSs while a reverse behavior is observed with EDSs. With the exception of NO_2, NO and CN substituents, the O*···H distance in TSHCs is shorter than that in BHCs. The strong EWD character of NO_2, NO and CN can be reason for increasing the O*···H distance in TSHCs. Therefore, the π-stacking interaction involved in TSHCs increases the hydrogen bonding capacity of MNP in the presence of EDSs and weak EWSs, while it decreases with the strong EWSs.

AIM analysis

AIM analysis on the wave functions generated at the M06-2X/6-311++G(d,p) level of theory has been carried out to investigate π-stacking interactions in terms of topological properties of electron charge density [25]. Typical molecular graphs of BSCs and TSHCs is presented in Scheme 2. Bond critical points (BCPs; red dots), ring critical points (RCPs; yellow dots), and cage critical points (CCPs; green dots) were illustrated in this graph.

The electron charge density calculated at the RCP, ρ_{RCP}, are also given in Table 2. For BSCs, reasonable correlations are observed between the ΔE values and ρ_{RCPS} of rings, (R = 0.93 for I, 0.96 for II and 0.95 for III) and the sum of ρ_{RCPs} calculated between two rings (R = 0.95 for I + II, 0.94 for I + III, and 0.96 for II + III).

The sum of electron densities calculated at the BCPs obtained between the rings are also presented in Table 2. The highest/lowest $\sum\rho_{BCP}$ value has been obtained in the presence of SH/OH substituent for BSCs. As can be seen in Table 2, the $\sum\rho_{BCP}$ values calculated between the rings of the complexes in the presence of EWSs are higher than those in the presence of EDSs (with the exception of SH and NH_2). A linear relationship is not observed between ΔE and some of topological properties of electron charge density. This can be generally attributed to the direct interactions substituents and the MNP ring; for example, a BCP is observed between the SH substituent and MNP unit in the Ph-X‖MNP complex. We found a correlation equation based on topological properties for prediction of the ΔE values of the complexes.

$$\Delta E_{Ph\text{-}X\|MNP} = -38.24\sum\rho_{BCP} - 25.88\sum\rho_{RCP} + 167.38 \quad (3)$$

$\sum\rho_{RCP}$ is the sum of electron charge density calculated at the ring critical points. As can be seen in Fig. 2, there is good correlation (R = 0.97, with the exception of X = H) between the calculated ΔE values and ΔE_{pred} values obtained from equations 3.

The hydrogen bond strength can be evaluated via the ρ_{BCP} value calculated at BCP of the hydrogen bond [26,27]. The magnitude of the ρ_{BCP} values calculated at the O*···H BCP in TSHCs are presented in Table 2. The highest and lowest values correspond to NH_2 and NO_2 substituents, respectively. The ρ_{BCP} values calculated in the presence of EWSs are lower than EDSs. On the other hand, to investigate the π-stacking effects on the hydrogen bonding capacity of MNP, the ρ_{BCP} value calculated at the O*···H BCP in BHCs is compared with that of TSHCs. As shown in Table 2, the magnitude of the ρ_{BCP} value calculated at the O*···H BCP in TSHCs is higher than that in BHC (with the exception of NO_2, NO and CN). The higher ρ_{BCP} values indicates that the π-stacking interaction involved in TSHCs increases the hydrogen bond interaction. An excellent relationship between the ρ_{BCP} values and $R_{O\cdots H}$ (R = 0.99; see supplementary material, Fig. S2) has been identified.

ESP analysis

The ESP values can be used as a reliable descriptor of the hydrogen bond strength [28,29]. A more negative electrostatic potential leads to stronger electrostatic interactions with hydrogen bond donors [30-33]. Thus, the sum of local minima of ESPs calculated between rings and the global minimum of ESP, V_{min}, that corresponds to the O* atom of the stacked MNP in BSCs, as a measure of hydrogen bonding ability, were calculated by Multiwfn 3.2 package (see Table 3). Also, a typical ESP mapped molecular vdW surface of BSC is shown in Scheme 3.

The results show that the lowest and highest values of $|V_{min}|$ correspond to NO_2 and NH_2 substituents, respectively. The V_{min} values become more negative with EDSs in comparison with the unsubstituted case while a reverse behavior is observed for EWSs. These results are in agreement with the ρ_{BCP} values calculated at the O*···H BCP in TSHCs. The more negative V_{min} values are accompanied with the higher ρ_{BCP} values, so, the V_{min} around the O* atom of the stacked MNP can be used as a measure of hydrogen bonding ability in BSCs.

Furthermore, ∑ESPs calculated between the substituted benzene and MNP can be used as a descriptor for interplay between π-stacking and H-bonding ability. As can be seen in Table 3, the most positive/negative value of ∑ESP is observed in the presence of NO_2/NH_2 substituent for BSCs and TSHCs. Substitution with both the ED and EW substituents (with the exception of NH_2) decreases the ∑ESPs values between the rings in comparison with the unsubstituted case. It is important to mention that the positive values of ∑ESP correspond to NO_2, NO and CN substituents and their values become more positive after the O*···H H-bond formation. The ∑ESP values correlate well with the changes in the O*···H bond length and ρ_{BCP} value calculated at BCP of that bond (see Fig. 3, R = 0.93).

Also, there is a linear correlations between the ∑ESPs calculated between two rings and V_{min} calculated around the O* atom in BSCs (see Fig. 4). Thus, the H-bonding ability can be related to the sum of local minima of ESPs calculated between rings in these complexes.

The Hammett constants [34,35] correlate with the electronic effects of the substituents, which can herein affect the V_{min} values around the O* atom. As can be seen in Table 3, both EW and ED substituents (with the exception of NH_2) decrease V_{min} around the O* atom, where the effect is more obvious with EWSs. Thus, the ESP values depend on the nature of the substituents. Herein, good correlations are observed for σ_{meta}–V_{min} and σ_{meta}–∑ESP pairs in BSCs (see Fig. 5). It shows

that the Hammett constants can be used in the prediction of ESP and ∑ESP values of BSCs. Also, good relationships are observed for ∑ESP-ρ_{RCP} (calculated for rings I, II or III) and ∑ESP-∑ρ_{RCP} (calculated for rings I or II pairs).

NPA analysis

The NPA charges have been calculated using the densities obtained at the M06-2X/6-311++G(d,p) level of theory. The charge transfer (CT) has been estimated on the basis of the sum of atomic charges (∑q) calculated on the fragments of BSCs. With respect to the ∑q values reported in Table 4, CT occurs from MNP to Ph-X fragment. In the presence of EDSs, CT to Ph-X is lower than that of EWSs. Higher CTs to Ph-X fragment are accompanied with the lower ESP values around the O* atom and the lower hydrogen bonding ability of BSCs. Also, CT to HF molecule in TSHCs has been calculated on the basis of the sum of atomic charges calculated on the HF molecule ($\sum q_{HF}$). With respect to the $\sum q_{HF}$ values (see Table 4), CT to HF increases in the presence of EDSs while a reverse behavior is observed for EWSs. The highest/lowest CT corresponds to NH_2/NO_2 substituent. Also, an excellent correlation was found between CT and ρ_{BCP} values calculated at the O*···H BCP in TSHCs (see Fig. 6, R = 1.0). Thus, the hydrogen bond strength increases by increasing CT to HF molecule in TSHCs. As can be seen in Table 4, the CT value in TSHCs is more than that in BHC (with the exception of the NO_2, NO and CN substituents). So, the O*···H H-bond strength increases in the presence of EDSs and weak EWSs, while it decreases with the strong EWSs.

The donor-acceptor interaction energy E^2 of the $lp_{O*} \rightarrow \sigma^*_{HF}$ interaction can be used as a measure of the strength of O*···H hydrogen bond; the E^2 values obtained from the NBO analysis are given

in Table 4. The results show that the highest/lowest value corresponds to NH_2/NO_2. The E^2 values increase/decrease in the presence of EDSs/EWSs. Also, to investigate π-stacking effects on the hydrogen bonding stability of MNP, the E^2 values of $lp_{O^*} \rightarrow \sigma^*_{HF}$ interaction in TSHCs were compared with that in BHC. The E^2 values of $lp_{O^*} \rightarrow \sigma^*_{HF}$ interaction in TSHCs are more than that in BHC for EDSs and weak EWSs. This result is in agreement with the data obtained from the AIM analysis. Also, there is an excellent correlation between the E^2 values of $lp_{O^*} \rightarrow \sigma^*_{HF}$ interaction and CT to HF molecule in TSHCs (R = 1.0; see supplementary material, Fig. S3).

The C=O* bond dipole moment (μ) is important in biological activity of MNP, where the interaction of this molecule with biomolecules can be developed by hydrogen bonding of the carbonyl group and van der Waals forces. The μ values calculated for C=O* bond in BSCs are given in Table 4. The lowest μ value corresponds to the NO_2 and NO substituents and the highest μ value corresponds to the NH_2 substituent. EWSs decrease the μ values, while EDSs increase that. So, EDSs may lead to a stronger dipole–dipole interaction of the stacked MNP with the biomolecule active sites. The effect of substituents on μ has been investigated via the relationship between μ and the electronic parameters of the substituents (σ_{Para} and σ_{meta}). The results show that there are linear relationships between μ and the electronic parameters of substituents (R = 0.95 for σ_{Para}, R= 0.90 for σ_{meta}; see supplementary material, Fig. S4). In addition, reasonable linear correlations are observed for pairs of μ with the charge calculated on the O* atom (R = 0.98; see supplementary material, Fig. S5) and the ∑ESP values calculated between the rings in BSCs (see Fig. 7, R = 0.91 with the exception of H).

Also, the μ values calculated for C=O* bond in TSHCs are given in Table 4. The results show that the μ values increase by the hydrogen bond formation in TSHCs, where the growth is higher with EDSs. On the other hand, an excellent correlation was found between the μ values calculated for

C=O* bond and the ρ_{BCP} values calculated at the O*···H BCP in TSHCs (see Fig. 8, R = 0.94). The μ values calculated for the C=O* bond of the stacked MNP can be used as a measure of hydrogen bonding ability in BSCs.

The qO* values (see Table 4) in the presence of EWSs is less negative than those in the presence of EDSs. An approximately linear relationship is observed between qO* and V_{min} (R = 0.90) and ∑ESP (R = 0.91) values. Furthermore, a good linear correlation (R = 0.96) is found between qO* values and σ_{meta} (see Fig. 9, with the exception of H).

Conclusions

The influence of π-stacking interaction of substituted benzenes with fused six membered system of methyl 2-naphthoate (MNP) on the hydrogen bonding ability of -CO group of MNP is detectable with the quantum mechanical calculations. The results show that all substituents, regardless of their EW or ED character, increase the π-stacking interaction energies, where the change is higher in the presence of EWSs. A combination of the σ_{meta}, σ_{para} and MR values were fitted with the π-stacking interaction energies.

According to the AIM analysis, the $\sum\rho_{BCP}$ values of the BCPs obtained between rings in BSCs in the presence of EWSs are higher than EDSs, which is in agreement with the energy data. A correlation equation based on the topological properties of electron charge density was found for prediction of the ΔE values. The results indicate that the π-stacking interaction increases the ρ_{BCP} value at the O*···H BCP in TSHCs. The O*···H bond length decreases with increasing the ρ_{BCP} value.

The ESP values can be used as a measure of the hydrogen bond strength in BSCs. The V_{min} values become more negative with EDSs in comparison with the unsubstituted case while a reverse behavior is observed for EWSs. A good correlation is observed between V_{min} around the O* atom in BSCs and the ρ_{BCP} value in TSHCs. The positive values of ∑ESP calculated between two rings correspond to NO_2, NO and CN substituents and their values become more positive after the hydrogen bond formation. On the other hand, the ∑ESP values correlate well with the changes in O*···H bond length and the ρ_{BCP} of this bond. Also, good correlations are observed for σ_{meta}–V_{min} and σ_{meta}–∑ESP pairs in BSCs.

The NPA analysis show that there is a significant CT from lone electron pairs of O* atom to the HF molecule in TSHCs and BHC. The value of CT in TSHCs is more than that in BHC. CT correlates very well with the ρ_{BCP} value at the O*···H BCP in TSHCs. π-stacking effects on the hydrogen bonding capacity of MNP can be determine by comparing the E^2 value of $lp_{O^*} \rightarrow \sigma^*_{HF}$ interaction in TSHCs and BHC. The results show that the E^2 value of $lp_{O^*} \rightarrow \sigma^*_{HF}$ interaction in TSHCs is more than that in BHC for EDSs and weak EWSs. Furthermore, an excellent correlation was found between q_{O^*} and σ_{meta}.

EWSs decrease the C=O* bond dipole moment (μ), while EDSs increase that. Therefore, EDSs may lead to a stronger dipole–dipole interaction of MNP with the biomolecules active sites. Also a good correlation is observed between μ and ∑ESP values calculated between stacked rings.

Acknowledgment

We thank the university of Sistan and Baluchestan for financial supports and Computational Quantum Chemistry Laboratory for computational facilities.

References

1. M.L. Waters, Aromatic interactions in model systems, Curr. Opin. Chem. Bio 6 (2002) 736–741.

2. C.A. Hunter, K.R. Lawson, J. Perkins, and C.J. Urch, Aromatic interactions, J. Chem. Soc. Perkin Trans. 2 (2001) 651–669.

3. K.M. Dethlefs, and P. Hobza, Noncovalent interactions: A challenge for experiment and theory, Chem. Rev. 100 (2000) 143–167.

4. E.A. Meyer, R.K. Castellano, and F. Diederich, Interactions with aromatic rings in chemical and biological recognition, Angew. Chem. Int. Ed. 42 (2003) 1210–1250.

5. P. Hobza, Stacking interactions, Stacking interactions, Phys. Chem. Chem. Phys. 10 (2008) 2581–2583.

6. C.A. Hunter, and J.K.M. Sanders, The Nature of π-π Interactions, J. Am. Chem. Soc. 112 (1990) 5525–5534.

7. P. Mignon, S. Loverix, F.D. Proft, and P. Geerlings, Influence of Stacking on Hydrogen Bonding: Quantum Chemical Study on Pyridine-Benzene Model Complexes, J. Phys. Chem. A. 108 (2004) 6038–6044.

8. P. Mignon, S. Loverix, and P. Geerlings, Interplay between π–π interactions and the H-bonding ability of aromatic nitrogen bases, Chem. Physic. Lett. 401 (2005) 40–46.

9. P. Mignon, S. Loverix, J. Steyaert, and P. Geerlings, Influence of the pi-pi interaction on the hydrogen bonding capacity of stacked DNA/RNA bases, Nucleic Acids Res. 33 (2005) 1779–1789.

10. Z. Rua, and G.X. Wang, Methyl 1-bromo-2-naphthoate, Acta. Cryst. 65 (2009) 3264.

11. P. Ertl, S. Jelfs, J. Muhlbacher, A. Schuffenhauer, and P. Selzer, Quest for the Rings. In Silico Exploration of Ring Universe To Identify Novel Bioactive Heteroaromatic Scaffolds, J. Med. Chem. 49 (2006) 4568–4573.

12. C.F.H. Allen, Six-membered heterocyclic nitrogen compounds with four condensed rings, Interscience, New York-London, 1951.

13. Y. Zhao, and D.G. Truhlar, The M06 Suite of Density Functionals for Main Group Thermochemistry, Thermochemical Kinetics, Noncovalent Interactions, Excited States, and Transition Elements: Two New Functionals and Systematic Testing of Four M06-Class Functionals and 12 Other Functionals, Theor. Chem. Acc 120 (2008) 215–241.

14. M.J. Frisch, and et al., Gaussian 09, Revision A.02, Gaussian Inc., Wallingford, CT, 2009.

15. E.G. Hohenstein, S.T. Chill, and C.D. Sherrill, Assessment of the Performance of the M05-2X and M06-2X Exchange-Correlation Functionals for Noncovalent Interactions in Biomolecules, J. Chem. Theor. Comput. 4 (2008) 1996–2000.

16. S.F. Boys, F. Bernardi, The calculation of small molecular interactions by the differences of separate total energies. Some procedures with reduced errors, Mol. Phys. 19 (1970) 553 – 566.

17. K.F. Biegler, J. Schonbohm, D. Bayles, AIM2000-a program to analyze and visualize atoms in molecules, J. Comput. Chem. 22 (2001) 545–559.

18. A.E. Reed, R.B. Weinstock, and F. Weinhold, Natural population analysis, J. Chem. Phys. 83 (1985) 735–746.

19. E.D. Glendening, A.E. Reed, J.E. Carpenter, and F. Weinhold, NBO Version 3.1. Theoretical Chemistry Institute, University of Wisconsin, Madison, 1990.

20. T. Lu, F. Chen, Multiwfn: A Multifunctional Wavefunction Analyzer. J. Comput. Chem 33 (2012) 580–592.

21. C.A. Hunter, and J.K.M. Sanders, The nature of pi-pi interactions, J. Am. Chem. Soc. 112 (1990) 5525–5534.

22. M.O. Sinnokrot, and C.D. Sherrill, Substituent effects in π-π interactions: sandwich and T-shaped configurations, J. Am. Chem. Soc. 126 (2004) 7690–7697.

23. M. Watt, L.K.E. Hardebeck, C.C. Kirkpatrick, and M. Lewis, Face-to-face arene-arene binding energies: dominated by dispersion but predicted by electrostatic and dispersion/polarizability substituent constants, J. Am. Chem. Soc. 133 (2011) 3854–3862.

24. C. Hansch, S.D. Rockwell, P.Y.C. Jow, A. Leo, and E.E. Steller, Substituent constants for correlation cnalysis, J. Med. Chem. 20 (1977) 304–306.

25. C.F. Matta, N. Castillo, and R.J. Boyd, Extended weak bonding interactions in DNA: pi-stacking (base-base), base-backbone, and backbone-backbone interactions, J. Phys. Chem. B. 110 (2006) 563–578.

26. P. Popelier, Characterization of a dihydrogen bond on the basis of the electron density, The J. Phys. Chem. A. 102 (1998) 1873–1878.

27. X. Liang, X. Pu, H. Zhou, N.B. Wong, A. Tian, Keto-enoltautomerization of cya-nuric acid in the gas phase and in water and methanol, J. Mol. Struc. THEOCHEM. 816 (2007) 125–136.

28. P. Kollman, J.M. Kelvey, A. Johansson, and S. Rothenberg, Theoretical studies of hydrogen-bond dimers, J. Am. Chem. Soc. 97 (1975) 955–965.

29. P.S. Kushwaha, and P.C. Mishra, Relationship of hydrogen bonding energy with electrostatic and polarization energies and molecular electrostatic potentials for amino acids: An evaluation of the lock and key model, Int. J. Quantum Chem. 76 (2000) 700–713.

30. A. Baeten, F.D. Proft, and P. Geerlings, Basicity of primary amines: a group properties based study of the importance of inductive (electronegativity and softness) and resonance effects, Chem. Phys. Lett. 235 (1995) 17–21.

31. A. Baeten, F.D. Proft, and P. Geerlings, Proton Affinities of Amino Acids: Their Interpretation with Density Functional Theory based Descriptors, Int. J. Quantum Chem. 60 (1996) 931–940.

32. P.C. Mishra, and A. Kumar, Molecular electrostatic potentials and fields: hydrogen bonding, recognition, reactivity and modeling, Theor. Comput. Chem. 3 (1996) 257–296.

33. P.S. Kushwaha, and P.C. Mishra, Relationship of hydrogen bonding energy with electrostatic and polarization energies and molecular electrostatic potentials for amino acids: An evaluation of the lock and key model, Int. J. Quantum Chem. 76 (2000) 700–713.

34. L.P. Hammett, Some relations between reaction rates and equilibrium constants, Chem. Rev. 17 (1935) 125–136.

35. F. Cozzi, F. Ponzini, R. Annunziata, M. Cinquini, and J.S. Siegel, Polar interactions between stacked π systems in fluorinated 1,8-diarylnaphthalenes: Importance of quadrupole moments in molecular recognition, Angew. Chem., Int. Ed. 34 (1995) 1019–1020.

Table 1. Interaction energies (ΔE in kcal mol^{-1}) of BSCs and TSHCs at the M06-2X/6-311++G(d,p) level, the O*···H bond length ($R_{O\cdots H}$ in Å) in TSHCs, and the substituent constants

X	ΔE^{N}_{BSC}	ΔE^{N}_{TSHC}	ΔE^{B}_{BSC}	ΔE^{B}_{TSHC}	$R_{O\cdots H}$	σ_{meta}	σ_{para}	MR
NO_2	-9.21	-20.95	-7.24(1.97)	-18.06(2.89)	1.686	0.710	0.778	7.36
NO	-8.05	-19.48	-6.34(1.71)	-16.95(2.53)	1.684	0.620	0.910	5.20
COOH	-7.56	-19.27	-5.99(1.57)	-16.85(2.41)	1.681	0.370	0.450	6.93
SH	-7.41	-19.19	-5.73(1.68)	-16.72(2.47)	1.679	0.250	0.150	9.22
CN	-7.08	-19.72	-5.84(1.24)	-17.38(2.34)	1.682	0.560	0.660	6.33
Cl	-6.77	-18.20	-5.25(1.52)	-15.86(2.34)	1.681	0.373	0.227	6.03
NH_2	-6.56	-18.31	-5.12(1.44)	-16.03(2.27)	1.675	-0.160	-0.660	5.42
OH	-6.08	-17.63	-4.68(1.40)	-15.42(2.21)	1.679	0.121	-0.370	2.85
OCH_3	-6.07	-17.91	-4.59(1.48)	-15.61(2.30)	1.678	0.115	-0.268	7.87
H	-5.51	-17.12	-4.31(1.20)	-15.11(2.01)	1.679	0.000	0.000	1.03
BHC	**-10.55**	-	**-10.54(0.01)**	-	**1.682**	-	-	-

ΔE^{N} and ΔE^{B} represent the interaction energies without and with the BSSE correction, respectively. The data in the parentheses correspond to size of the BSSE correction for each complex. σ_{meta}, σ_{para} = Hammett constants; MR = molar refractivity (polarizability) constant. The substituent constants were obtained from a standard reference [24].

Table 2. The ρ_{BCP} values at the BCPs obtained between the rings, the $\sum\rho_{BCP}$ values calculated between the rings, the ρ_{BCP} values at the O*···H BCP of TSHCs and the ρ_{RCP} values calculated at the RCPs of rings I, II or III of BSCs at the M06-2X/6-311++G(d,p) level of theory in e/au^3.

X		$\rho_{BCP}\times10^{-2}$ BSC	$\sum\rho_{BCP}\times10^{-2}$ BSC	$\rho_{BCP}\times10^{-2}$ O*···H TSHC	$\rho_{RCP}\times10^{-2}$ BSC		
					I	II	III
NO_2	$C7_a\cdots N1_b$	0.412	2.565	3.965	2.297	2.198	2.203
	$C10_a\cdots C2_b$	0.537					
	$C1_a\cdots C3_b$	0.536					
	$C4_a\cdots C5_b$	0.541					
	$C5_a\cdots C6_b$	0.537					
NO	$C7_a\cdots N1_b$	0.376	2.078	3.978	2.289	2.196	2.202
	$C10_a\cdots C2_b$	0.542					
	$C4_a\cdots C5_b$	0.544					
	$C5_a\cdots C6_b$	0.554					
COOH	$C7_a\cdots C11_b$	0.389	2.279	4.019	2.279	2.194	2.200
	$C10_a\cdots C2_b$	0.468					
	$C1_a\cdots C3_b$	0.458					
	$C4_a\cdots C5_b$	0.481					
	$C5_a\cdots C6_b$	0.482					
SH	$C8_a\cdots S1_b$	0.521	2.708	4.046	2.261	2.193	2.201
	$C10_a\cdots C1_b$	0.539					
	$C1_a\cdots C2_b$	0.551					
	$C4_a\cdots C4_b$	0.559					
	$C5_a\cdots C5_b$	0.538					

CN	$C6_a\cdots C11_b$	0.327	1.912	3.999	2.253	2.193	2.201
	$C10_a\cdots C2_b$	0.394					
	$C10_a\cdots C3_b$	0.395					
	$C4_a\cdots C5_b$	0.399					
	$C5_a\cdots C6_b$	0.397					
Cl	$C7_a\cdots Cl$	0.414	2.045	4.022	2.261	2.190	2.199
	$C8_a\cdots C2_b$	0.401					
	$C10_a\cdots C3_b$	0.396					
	$C4_a\cdots C5_b$	0.411					
	$C5_a\cdots C6_b$	0.424					
NH_2	$C8_a\cdots N1$	0.442	2.092	4.089	2.235	2.192	2.199
	$C1_a\cdots C2_b$	0.550					
	$C4_a\cdots C4_b$	0.561					
	$C5_a\cdots C5_b$	0.538					
OH	$C10_a\cdots C2_b$	0.496	1.414	4.039	2.238	2.190	2.199
	$C4_a\cdots C4_b$	0.482					
	$C5_a\cdots C5_b$	0.436					
OCH_3	$H8_b\cdots H11_a$	0.211	1.661	4.055	2.236	2.191	2.199
	$C10_a\cdots C2_b$	0.476					
	$C4_a\cdots C4_b$	0.493					
	$C5_a\cdots C5_b$	0.480					
H	$C10_a\cdots C2_b$	0.464	1.886	4.035	2.264	2.190	2.198
	$C1_a\cdots C3_b$	0.460					
	$C4_a\cdots C5_b$	0.488					
	$C9_a\cdots C6_b$	0.474					
BHC	-	-	-	**4.002**	-	-	-

Table 3. The global minimum value of ESP calculated around the O* atom (V_{min} in kcal mol^{-1}) of BSCs and the sum of local minima of ESPs calculated between the rings (∑ESP in kcal mol^{-1}) in BSCs and TSHCs

X	V_{min} BSC	∑ESP BSC	∑ESP TSHC
NO_2	-31.746	9.867	22.256
NO	-32.746	2.679	15.364
COOH	-33.768	-25.737	-9.683
SH	-34.059	-30.869	-11.591
CN	-32.137	0.437	20.369
Cl	-33.969	-26.364	-1.016
NH_2	-35.898	-55.932	-32.157
OH	-33.617	-24.203	-13.119
OCH_3	-34.310	-34.431	-16.574
H	-35.069	-47.506	-20.117

Table 4. The sum of atomic charges (in e) calculated on the MNP in BSCs and on the HF molecule in TSHCs, the charge on the O* atom in BSCs, the dipole moment of C=O* bond (in debye) in TSHCs and BSCs and the E^2 values (in kcal mol^{-1}) of $lp_{O*} \rightarrow \sigma^*_{HF}$ interaction obtained from the NBO analysis in TSHCs

X	$\sum q$ BSC	$\sum q_{HF}$ TSHC	q_{O*} BSC	μ BSC	μ TSHC	$^aE^2$ TSHC
NO_2	0.0073	-0.0298	-0.612	3.184	3.606	20.73
NO	0.0094	-0.0300	-0.612	3.184	3.606	20.85
COOH	0.0050	-0.0306	-0.614	3.191	3.612	21.25
SH	0.0027	-0.0311	-0.615	3.197	3.620	21.54
CN	0.0053	-0.0303	-0.613	3.186	3.609	21.08
Cl	0.0011	-0.0308	-0.614	3.189	3.610	21.30
NH_2	0.0027	-0.0318	-0.616	3.204	3.632	21.98
OH	0.0026	-0.0310	-0.616	3.199	3.623	21.47
OCH_3	0.0027	-0.0312	-0.616	3.199	3.624	21.62
H	0.0047	-0.0309	-0.614	3.192	3.615	21.43
BHC	-	**-0.0306**	**-0.611**	**3.180**	**3.599**	**21.12**

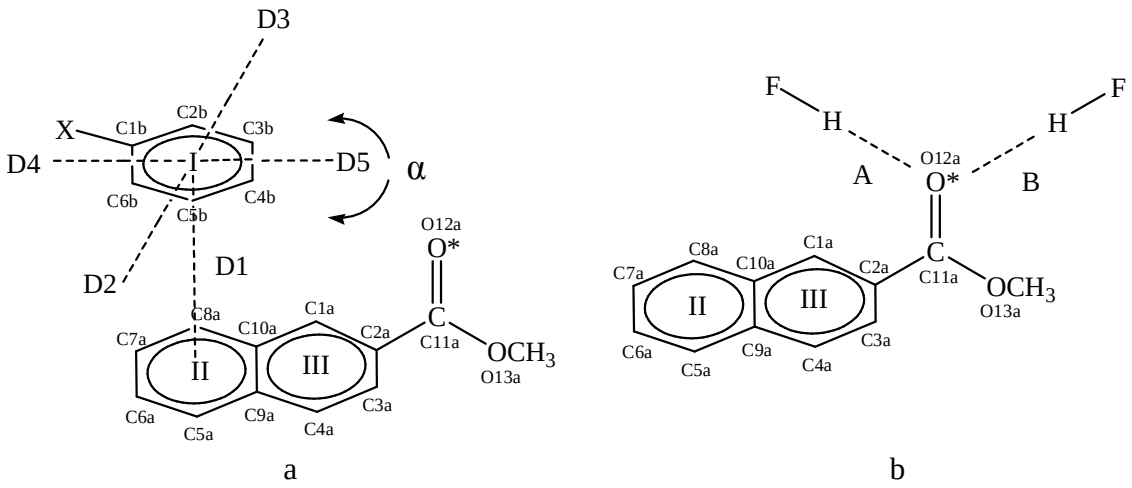

Scheme 1. (a) Definition of variables in BSCs with atomic numbering scheme. (b) Two orientations A and B for interaction of the HF molecule via hydrogen bonding in MNP.

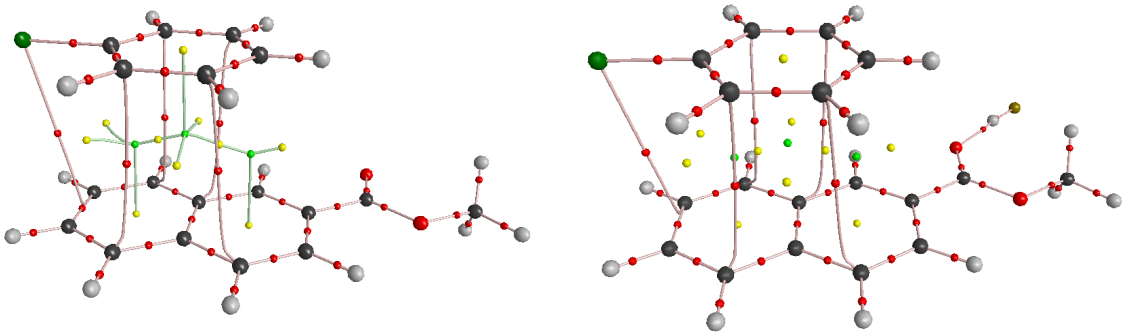

Scheme 2. Typical molecular graphs of BSCs and TSHCs. The small red, green, and yellow spheres correspond to BCPs, CCPs and RCPs, respectively.

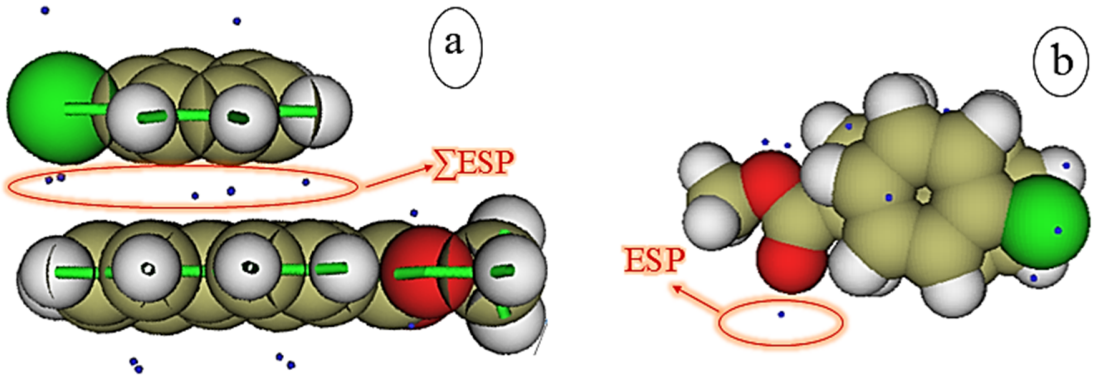

Scheme 3. The minimums on the surface of ESP of BSC. (a) The sum of the local minima of ESPs between two rings (∑ESP). (b) The global minimum of ESP (V_{min}).

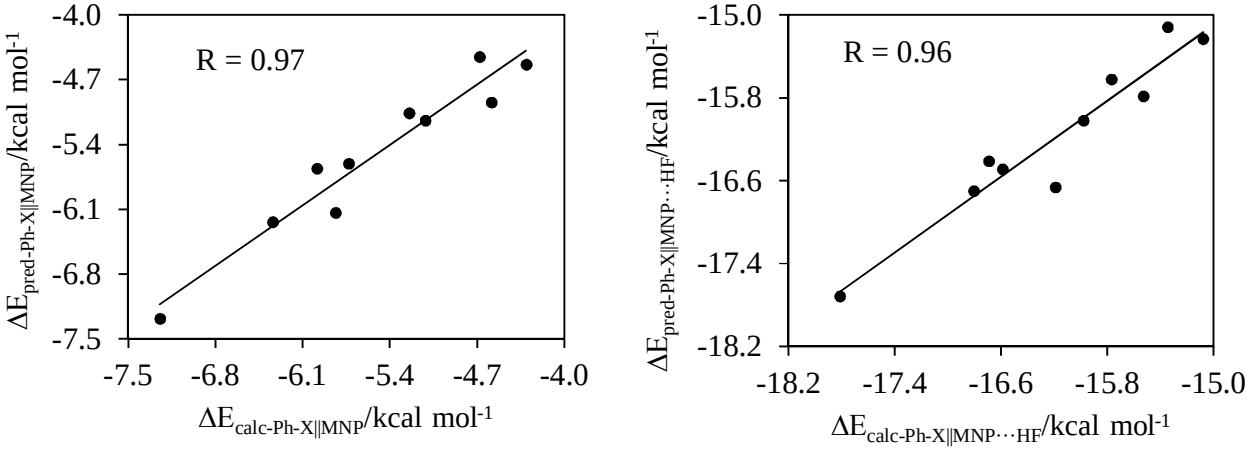

Fig. 1. Correlation between the ΔE values predicted by the equation and the ΔE values calculated from energy data.

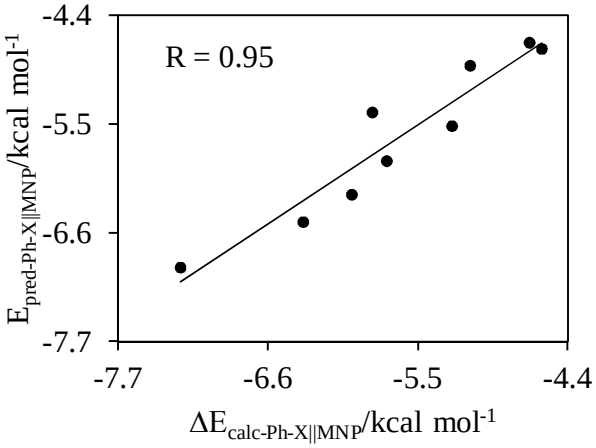

Fig. 2. Correlation between the ΔE values predicted by the equation, and the ΔE values calculated from energy data.

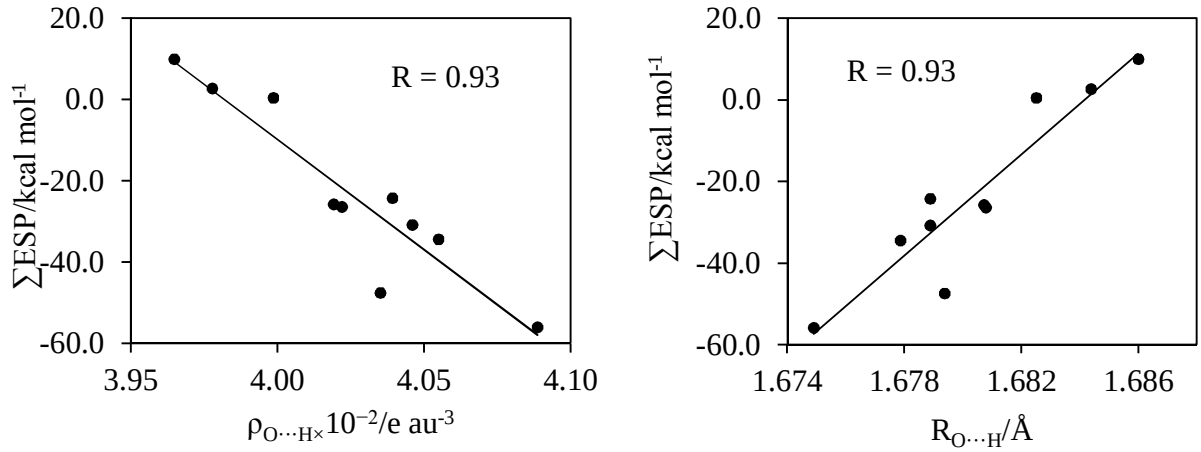

Fig. 3. Correlation of the ∑ESP values with changes in the ρ_{BCP} values and the O*···H bond length.

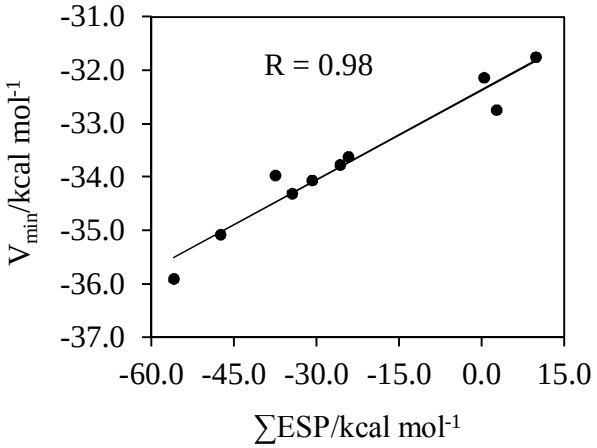

Fig. 4. Correlation between V_{min} calculated around the O* atom and the ∑ESPs calculated between rings.

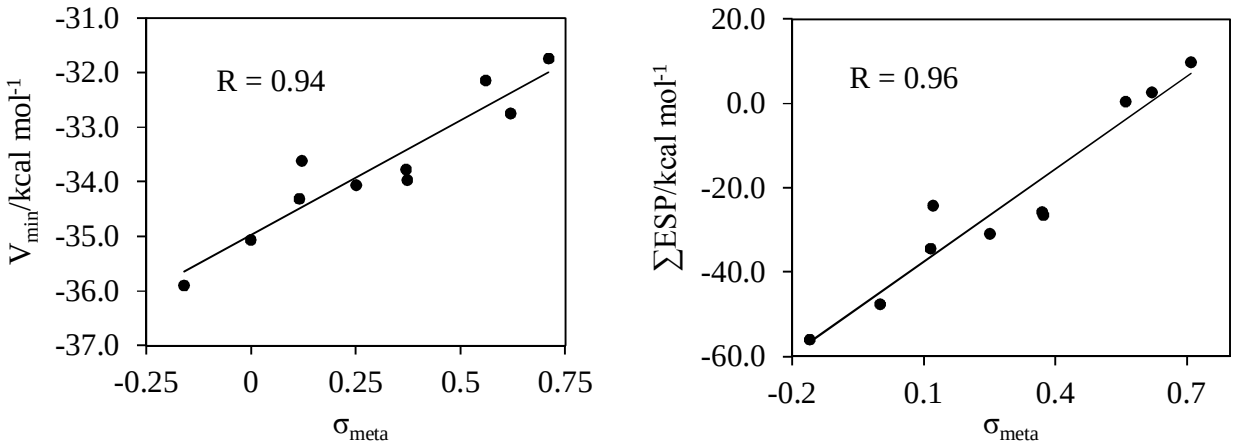

Fig. 5. Correlation of V_{min} calculated around the O* atom and the ∑ESPs calculated between rings with σ_{meta}.

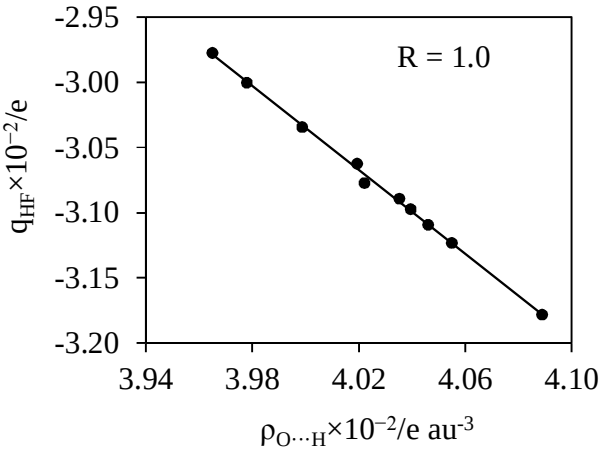

Fig. 6. Correlation between CT and the ρ_{BCP} values calculated at the O*···H BCP in TSHCs.

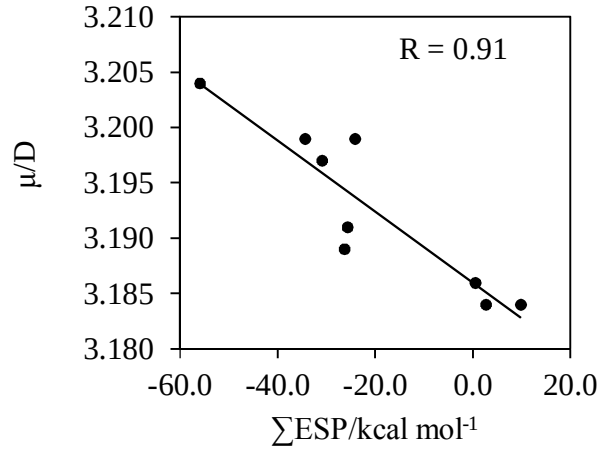

Fig. 7. Correlation between the ∑ESPs calculated between rings with dipole moment.

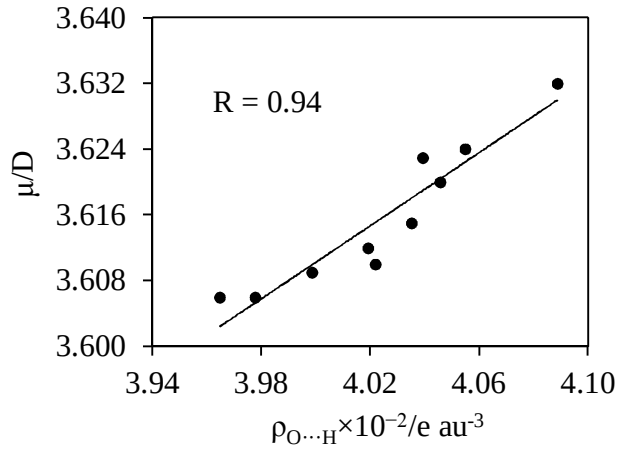

Fig. 8. Correlation between the μ values calculated for C=O* bond and the ρ_{BCP} values calculated at the O*···H BCP in TSHCs.

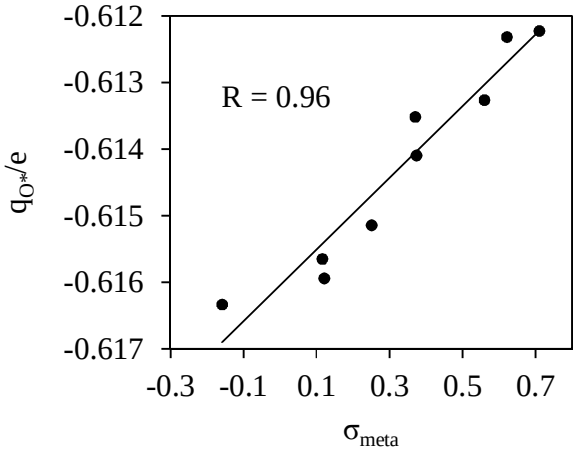

Fig. 9. Correlation between the natural charge calculated on the O* atom and σ_{meta}.